Review

Mechanical, Thermal, and Acoustic Properties of Hemp and Biocomposite Materials: A Review

Raj Kumar Dahal [1] , Bishnu Acharya [2] and Animesh Dutta [1,*]

1. Bio-Renewable Innovation Lab, School of Engineering, University of Guelph, Guelph, ON N1G 2W1, Canada
2. Department of Chemical and Biological Engineering, University of Saskatchewan, Saskatoon, SK S7N 5A9, Canada
* Correspondence: adutta@uoguelph.ca

Abstract: Bio-based products are paving a promising path towards a greener future and helping win the fight against climate change and global warming mainly caused by fossil fuel consumption. This paper aims at highlighting the acoustic, thermal, and mechanical properties of hemp-based biocomposite materials. Change in sound absorption as a result of hemp fibers and hemp particle reinforcement are discussed in this paper. The thermal properties characterized by the thermal conductivity of the composites are also presented, followed by the mechanical properties and the current issues in biocomposite materials mainly containing hemp as a constituent element. Lastly, the effects of biofillers and biofibers on the various properties of the hemp-composite materials are discussed. This paper highlights the development of and issues in the field of hemp-based composite materials.

Keywords: hemp fiber; thermal properties; mechanical properties; physical properties; acoustic properties; biocomposite material

1. Background

Glass–epoxy composite materials started being used in the 1950s during WWII [1] when mixtures were applied in mechanical structures, including boat hulls, sports car parts, and weaponry such as ballistic missile nose-caps, which replaced previous wooden components. The development of load-bearing structural parts began after the 1960s when the mechanical theory on laminate composites was proposed [1]. Epoxy–boron composites then started being used in structural applications for military and sports goods. Later, graphite/epoxy and aramid were developed as composites and used in structures while glass polymer composites started replacing steel and other metals in structural applications [2]. The expensive and rudimentary manufacturing techniques and processes used for these composites led to a saturation point in late 1980s [3,4]. Nevertheless, interest in and applications of composite materials have increased and evolved, with focus on manufacturing techniques, including injection molding, extrusion, and press molding [3].

By 2060, the global exponential population growth will more than double the estimated material resource demand. With current practices, this rise in material demand will have serious effects on the environment due to the tremendous amount of greenhouse gas (GHG) emissions and subsequent waste generation [5]. Therefore, focus has shifted to developing environmentally friendly bio-based composite materials. This is because plant-based products not only reduce GHG emissions to tackle global warming, but also reduce waste due to their biodegradability as well as improve peoples' health and quality of life. Hemp plants can provide food, paper, clothes, medicine, and strong bio-fibers. Hemp has been used in composite materials for centuries now. However, it presents challenges; hemp fibers contain a high level of moisture, as plant-based sources are hydrophilic in nature [6]. Additionally, its mechanical, thermal, and physical properties, such as tensile strength,

wettability, flammability, and swelling, vary. These properties change with changes in plant anatomy, fiber processing conditions, growth conditions, and experimental methods. This variation in properties is pivotal, as ununiform material properties will result in unpredictable product behaviours; concerns have been raised that they will promote material failures [7]. The drawbacks of hemp products can be improved upon, and they can be optimized by modifications, including thermal processing, blending with petroleum-based products, and incorporating biofillers. The biofillers in biomaterials help change their main characteristics, including their physical, mechanical, and thermal properties.

2. Present Status of and Challenges in Biocomposite Materials

Since the beginning of natural-fiber-reinforced plastic composites in the early 1900s, the need for bio-based products has been ever increasing. In the past, the low cost of oil hindered the progress of bio-based polymers. Nevertheless, the disruption and rocketing cost of the fossil fuel supplies, environmental awareness, and advancements in biotechnology have recently accelerated the promotion of bio-based polymers [8]. The global bioplastics market is estimated to reach USD 68.6 billion by 2024 [9]. It is a well-established fact that composites offer impressive and variable mechanical properties (better stiffness, tensile strength, improved hardness, and wear-resistance), thermal resistance, and attractive physical properties which are impossible or costly to achieve with pure metals/materials. Biomaterials and biocomposites are not a novel concept; however, there are technical issues that need to be addressed in order for plant-based sources to be included in composite systems. Despite the future market uncertainties, variation in properties, and economic hurdles, biocomposite research is continuing to substitute fossil fuel-based resources, aiming at utilizing renewable plant resources, which helps protect the environment, promote sustainability and renewability, and create jobs at the local level.

Since the complete replacement of fossil-based products is not feasible due to cost and performance, bio-based composite materials may have bio-based polymers, bio-based reinforcement, and fillers, or both, while having other ingredients from fossil fuel sources. As for reinforcement, nature can offer wooden and non-wooden fibers (bast, leaf, seed, core, grass, and reed) as composite reinforcements. Cellulosic non-wooden fibers offer tensile strengths ranging from 80 MPa for sisal to 938 MPa for ramie [10]. Applications of biocomposites in structures and infrastructures have proven useful in terms of their moderate mechanical properties, lower cost, availability, biodegradability, and environmental considerations.

Most previous and present studies only concentrate on the mechanical properties of composite materials. For instance, the electrical properties (resistivity and dielectric constant) of biopolymers are still understudied. Similarly, studies of biomatrices and biofibers, even those at present, apply empirical methods to determine the optimum proportions to produce a given specified composite material. The mathematical modelling of biocomposite materials to study various physical properties, including but not limited to thermal, mechanical, and acoustical properties, is still an unexplored area in the materials field.

For the characterization and classification of materials, the mechanical properties of polymer-based biocomposites have been widely explored. For instance, apart from being used in sofas and seats, coir fiber has shown impressive durability and weather-resistance when reinforced with concrete panels. Kenaf, ramie, roselle, and flax seed in their polymer-matrix composite forms have been studied for their mechanical properties with potential applications in auto parts, mechanical gears and parts, sockets for prostheses, and eco-friendly brakes. The good tensile strength of jute fibers and hemp fibers has been utilized in structural applications and in agriculture, aerospace, automobiles, construction, sports, domestic products, and auto parts to absorb noises due to their better sound-absorption [10].

In contrast, petroleum-based polymer matrices and inorganic fillers still dominate the composite industry. One of the main reasons that bio-products do not corner the market as expected is the uncertainty that lies in the research of biocomposite materials. Further hinderances to marketability include the hesitation to readily implement new technologies,

nonuniform filler and fiber properties, high moisture sensitivity, the low thermal stability of natural fibers and fillers, the up-scaling problem, and unproven production techniques.

2.1. Biofillers in Biocomposite Materials

Plant-sourced materials are renewable, sustainable, and abundantly available in nature. Apart from the applications of virgin bio-based polymers (PLA, PHAs, Bio-PBS, epoxy from lignin, and epoxied oil) and biodegradable petroleum-based (PCL, PBS and PBAT) polymers, scholars are interested in composites with bio-fibers and biofillers and emphasize the importance of their physical properties; the aim is to tackle environmental challenges as well as material failures due to the high moisture content, the hydrophilicity of bio-fibers, true and artificial variability in properties such as tensile strength, wettability, flammability, and swelling due to plant anatomy, fiber-processing conditions, and growth conditions. Plant-based fillers can be in powdered form or granular form, and short fibers or continuous fibers. A schematic diagram of the hand layup technique to prepare polymer–hemp composites with biocarbon fillers is shown in Figure 1.
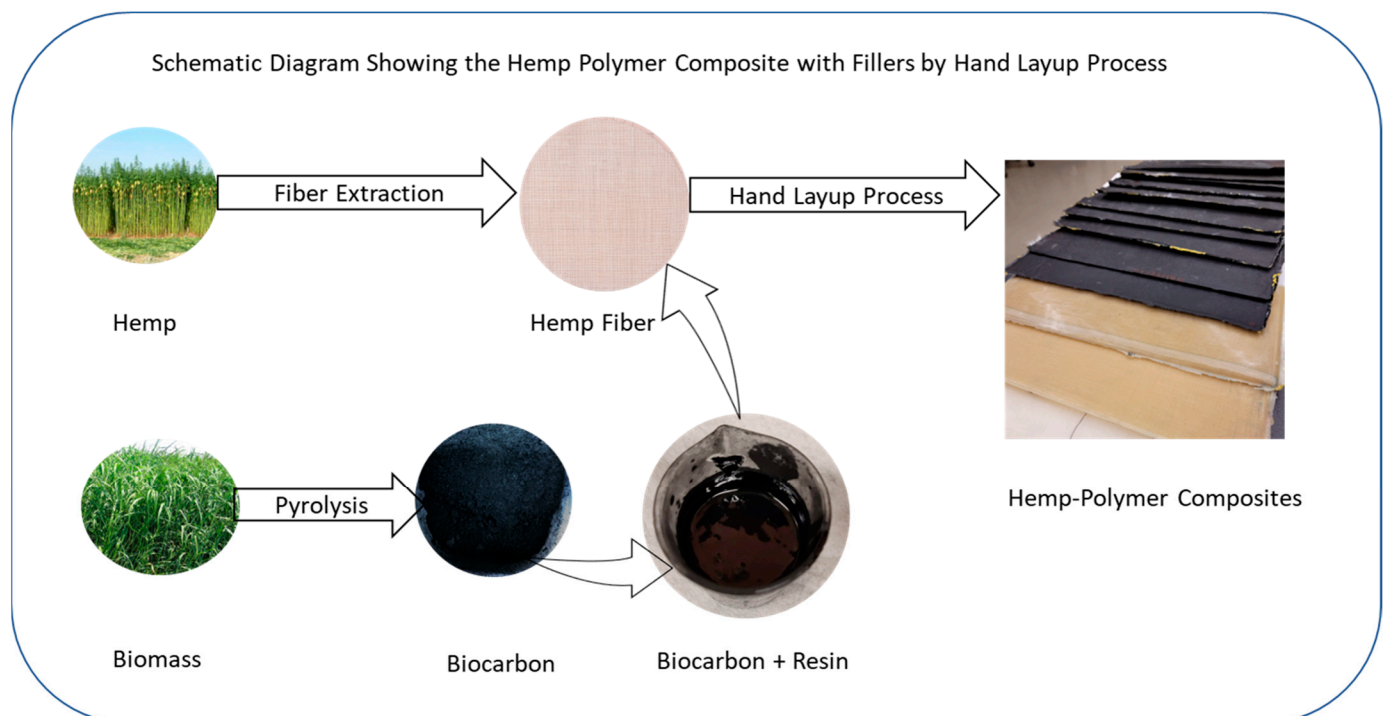
Figure 1. Showing the schematic of the preparation of hemp-polymer composites with fillers by hand layup technique.

Sun W. et al. studied the potential application of hemp-derived biocarbon in super-capacitor cells. An impressive specific capacitance of 160 F/g and an energy density of 19.8 Wh/kg at a power density of 21 kW/kg were reported [11]. Another attempt to enhance the electrical properties of an epoxy resin composite with the addition of biochar obtained from coffee waste was performed by Mauro Giorcelli and Mattio Bartoli [12]. Even though its performance was not comparable to that of the carbon-black-filled composites, it was found that the biochar from the coffee waste improved the electrical conductivity of the polymer composite materials when compared with the composites without fillers [12]. In a similar study, Nan N. et al. [13] demonstrated that the biocarbon in polyvinyl alcohol lowers its tensile strength and storage modulus below the composite's glass transition temperature. The authors claimed that there is a potential for the replacement of carbon nanotubes and graphene as a filler in electrical applications of polymers. Organic fillers sourced from various plant (rice husk, walnut shell, coconut shell) fibers in the form of particulate fillers in bio-epoxy resin and hardener have been tested by Chandramohan D.

and Presin Kumar A.J. [14]. The authors studied the mechanical properties as well as the effect of water on the mechanical strength of the composite samples. The hybrid composite samples showed a better flexural strength under wet conditions as compared to that of the dry samples. The walnut- and coconut-containing samples showed the least water absorption and a superior tensile strength (68.8 MPa), flexural strength (14.9 MPa), and shear strength (81.92 MPa). The value for the elongation at break (21.82%), the energy absorbed during the impact test (20.9 MPa), and the breaking load in the tensile and flexural tests of the composite samples with the walnut and coconut shells were also better than those of the composites with rice husk and coconut-shell fillers as well as rice husk and walnut-shell fillers. Abdellatef Y. et al. added hemp with a size of less than 6.3 mm to concrete to produce hempcrete and study its water-buffering capacity, as well as its mechanical and thermal behaviours [15]. The specific heat capacity of the hempcrete block was in the range of 1365 J/kg K to 1508 J/kg K. The results suggested its potential use for filling in walls. Thus, organic fillers in composite materials can help optimize their mechanical, electrical, thermal, and physical properties [16].

2.2. Role of Fiber in Resultant Material Properties

During the developmental phase, the desired properties of a composite material have been found to be dependent upon the type [17–19], orientation [20–26], size [27–31], and properties of the matrix as well as the reinforcement. Hemp fibers in composite materials come with different physical properties (aspect ratios), as well as mechanical, thermal, and chemical properties [32–37]. These properties are crucial, as the strength and properties of a fiber-reinforced composite depend on the alignment and size of these fibers. The fibers are aligned in the direction of the load so that a partial load is carried by the fiber which adds to the tensile strength and stiffness of the material in the principal stress direction [38–41]. This shows that the change in the fiber alignment can influence not only the strength and stiffness but also the impact toughness and shear modulus of the final material. In addition to that, the average strain sustained by the matrix and fiber in a continuous-fiber composite is similar, as they are collinear [38]. In contrast, the stress is unevenly distributed from fiber to fiber in short- and various-sized fiber composites [42–46]. Moreover, the stress concentration closer to the fiber ends in the composite results in an incomplete (semi-developed) stress distribution profile which weakens the composite materials due to the poor load-bearing capacity. The shear stress transfer mechanism is defined by the shear lag theory [47–49] which assumes the fibers are in tension and the matrix is in shear stress when a force is applied to the material. As a result, the stress rises from zero at the ends of the fiber to the maximum value at the midpoint (such as the load distribution in a simply supported beam). However, short fiber composites can have similar mechanical properties to those of continuous fiber composites if the short fibers are properly aligned, are well bonded with the matrix, and are longer than the critical length [44,50]. Another benefit of employing short fibers in composites is that they offer complex shapes through continuous or semi-continuous production processes, saving production costs and time [51–55]. This explains why fiber length is another important physical property of the fiber that affects the materials' properties. The properties of matrices and production techniques [56–60] are other factors that govern fiber selection for specific applications of composite materials. Once the material design based on the tensile behaviour of the fiber/matrix is accomplished, other factors that play significant roles in material characterization and classification include: the materials' heat resistance behaviour, production costs [61], tool wear [62,63], product density [64,65], and the compatibility between tools and equipment. For instance, the varying thermal properties of the fiber and the matrix can cause internal stresses due to thermal cycles sustained during material processing and production [66].

2.3. Hemp and Biocomposite Materials for Acoustic Properties

Due to their porous nature, the plant-based ingredients used in biomaterials improve the sound absorptivity by adding and changing the biofiller content in the matrices of

biocomposite materials [67,68]. Jiayi Guo (2016) [69] studied hemp residue with plastic polymers with different compositions and varying sound frequencies and found that the increased amount of hemp enhances the damping ability of the resulting material and hence the sound absorption due to its high-porosity nature. There have been other sound absorption studies of bio-based products, including the following: luffa fiber was studied by Hasan Koruk, Garip Genc (2019) [70]; PLA was studied by Yao R et al. (2016) [71] and Mosanenzadeh SG et al. (2014) [72]; pinewood fiber, rice straw, and pulp were studied by DT Liu et al. (2012) [73]; wool in composites was studied by Merve Kucuk and Yasemin Korkmaz (2012) [74]; poplar wood was studied by Limin Peng et al. (2014) [75]; nano clay was studied by R. Gayathri (2013) [76]; coir was studied by Zulkifli R et al. (2008) [77]; tea leaf fiber was studied by Seçkin Çelebi and Haluk Küçük (2012) [78]; meranti wood dust was studied by Sa'adon S and Rus AZM (2014) [79]; hemp, flax, beech, pine, and rapeseed straw were used to make lignocellulosic materials by Ewa Markiewicz, Dominik Paukszta and Sławomir Borysiak (2012) [80]; corn cobs, sunflower stems, and sheep wool were studied by Irina Oancea (2018) [81]; and hemp and kenaf fiber were studied by B. Yeşim Buyukakinci, Nihal Sokmen, and Haluk Kucuk (2011) [82]. In all these reinforcements, the matrices were plastic. From these findings, it was understood that the increase in the fiber matrix would increase the coefficient of the sound absorption. It has been reported that musical instruments made from glass fiber and from hemp perform in a similar fashion. Increasing the thickness of the natural fibers and introducing the fillers have been shown to reduce the noise reduction coefficient. Similarly, the noise reduction coefficient was found to increase with the reduction in filler sizes. These findings are derived from the summary in Table 1.

Hui Z. and Fan X. (2009) studied the sound-absorption properties of hemp fibrous assembly absorbers. They found that the sound absorption increased with increases in the thickness, bulk density, and air gap of the assembly as expected, while the sound absorption decreased by increasing the fiber diameter. When compared with wool, cotton, and acrylic fibers, hemp had an excellent performance due to its larger fiber diameter [83]. Buksnowitz C. et al. (2010) reinforced epoxy polymers with hemp and glass fibers to compare their sound absorptivity and found that the logarithmic acoustic damping for hemp was 0.0032 as compared to 0.0317 for glass fiber, indicating hemp composite's better sound absorption [84]. The acoustical properties of hemp-based materials were further studied by Jalil M. et al. (2014) using longitudinal, flexural free vibration, and forced vibration methods. Hemp-reinforced polyester composites demonstrated a significantly low acoustic conversion efficiency compared with that of carbon fiber polyester and glass fiber polyester composites. The acoustic conversion efficiency is a parameter used to evaluate the acoustic performance of a material based on its acoustic coefficient and sound quality factor. With such properties, hemp composites have applications in sound absorption while mineral-based composites are suitable for musical instruments [85]. Moreover, hemp shiv was solely studied by Gle P. et al. (2012) for its acoustical properties, showing a transmission loss lower than 10 dB with a material thickness of 5 cm [86] as compared to 43 dB with a 31 cm thickness when used in structures as hemp concrete bricks [87]. Furthermore, hemp concrete (two kinds of clay and hemp shiv) was examined for its acoustic performance in buildings, showing promising sound absorption and transmission loss [88]. Hemp has been gaining more attention as a building material recently. Fernea R. et al. (2019) performed another experiment to study hemp cement's acoustic properties and found that hemp fiber is a better thermal insulator than hemp shiv in all frequencies ranging between 250 and 4000 Hz. The sound absorption coefficient increased with the increase in sound frequency. With a multilayered composition, the concrete showed impressive sound absorption of up to 90% at a frequency range of 0 to 500 Hz [89].

Table 1. Biofiber-reinforced material for acoustic properties.

Ref.	Materials	Method	Findings
[69]	Hemp crop residue + Reclaimed crushed tire CT) + LDPE/PP.	The impedance tube method according to ASTM E1050-12.	The maximum sound absorption value of 0.68 at 1650 Hz for a 80% hemp hurd, 10% coarsely crushed tire, and 10% PP composite was found. A comparison showed whole stalk hemp (WSH) composites are better at damping acoustics than the rest; this could be due to the high porosity of WSH composites. The 30% WSH, 60% CT, and 10% LLDPE composite had the highest sound-absorption coefficient (α).
[70]	Luffa fibers w/o surface treatment + epoxy resin.	Absorptivity was measured using the impedance tube as per ASTM E1050-12 and the transmission loss levels as per ASTM E2611-17.	The value of α changed with the change in the fiber-matrix volume fraction. α decreased when the volume fraction of resin was further increased after a specific fiber-matrix ratio. Similarly, the transmission loss increased by increasing the matrix fraction. The transmission loss value of luffa composite with a 1.5 matrix volume fraction was found to be similar to that of a cement and glass plate.
[90]	Pinecone char (PCC)/China Poplar char (CPC) + Epoxy resin (ER) (10, 20 30 wt.%) + Poly pox Hardener 043 + (2,4,6-tris) dimethyl amino-methyl phenol catalyst.	Velocity was calculated from the equation of motion, and the acoustic impedance was calculated as $Z = \rho.V_L$, in which ρ is the material density and V_L is the longitudinal wave velocity.	The V_L of the ER/char composites was higher than that of pure ER. The V_L of the ER/CPC composites ranged from 2754 to 2811 m/s^2, while that of the ER/PCC composites ranged from 2726 to 2798 m/s^2. The biochar increased the acoustic impedance in all composites as compared to the pure ER. The velocities showed a linear increment with an increasing biochar concentration (PCC and CPC) in the ER/BC composites up to 30% due to the increased filler density and reduced inter-atomic spacing among the fillers.
[85]	Isophthalic unsaturated polyester resin + Methyl ethyl ketone peroxide (1 wt.%) and cobalt octoate (0.9 wt.%) + (Carbon fiber/Glass fiber/Hemp fiber).	Longitudinal and flexural free vibration tests were performed to analyze the acoustic response using the fast Fourier transform (FFT) method on MATLAB. A standard water absorption test was performed.	The glass-fiber-reinforced composites showed an acoustic performance similar to that of walnut wood. The carbon fiber-reinforced composite showed improved acoustical properties. The surrounding atmosphere's water content had a neglible effect on the quality of sound from instruments made from carbon fiber and glass fiber composites.
[73]	Pinewood fibers/Rice straw pulp + Polyurethane (PU) + Acetone/Acetic ether.	The impedance tube method was used according to ISO E10534-2. Sound frequencies from 90 to 7000 Hz were analyzed.	Void volume is a critical factor in damping sound. Wood fiber and straw fiber biocomposites have good sound-absorbing properties due to their better sound-absorbing behaviour over a wide frequency range (250 to 7000 Hz). The increase in fiber thickness lowered the value of the sound absorption coefficient (α). The compact-structure wood-fiber biocomposite offered a higher value of α compared to that of the straw fiber biocomposite of a similar thickness.
[91]	Polyethylene terephthalate (PET)/Lightweight microfibers/Blown plastic fibers/Glassfiber/blends of cotton or plastic fibers (shoddy) + Polyester/Polypropylene.	The sound absorptivity of the composites was determined according to ASTM E1050.	α was indirectly proportional to the fiber diameter, and the absorptivity increased with the increase in the specific flow resistance per unit thickness of the sample up to 1000; beyond this resistance value, α started to decrease. The tortuosity mainly influenced the location of the peaks, and the porosity and flow resistivity affected the size of the waves. Having a higher fiber surface area and a lower fiber size increases the value of α. Less-dense materials absorbed the sound of low frequencies (500 Hz), and highly dense composites absorbed waves above 2000 Hz. The air gap increased α for medium and higher frequencies. Attaching thin films such as PVC increased the α for low- and mid-frequency sounds.

Table 1. *Cont.*

| Ref.	Materials	Method	Findings
[92]	Biochar + (sand/coarse aggregate + cement powder in 3:1) + water.	The sound absorption coefficient (α) was determined using a Kundt tube as per ISO 10534-2. The noise reduction coefficient (NRC) was calculated as an average value.	The higher sound energy dissipation within the interconnected pore networks in the concrete by adding biochar caused higher sound absorption coefficients. Biochar showed similar effects to that of the activated carbon. Due to the high surface area and porosity of the activated carbon, the concrete with a higher amount of biochar resembled the concrete with a lower amount of activated carbon. The noise reduction did not change with the change in the carbon filler amount in the samples whereas it substantially affected the sound absorptivity of the final material.
[74]	7:3 wool and bicomponent (polyester Core with Co-polyester Sheath polyester: 7:3 cotton and polyester. 7:3 acrylic–cotton–polyester and polypropylene. 9:1 polyester and low melt polyester. 7:3 polyester and polyamide. Polyester only. meta-aramid only.	Sound absorption was measured at frequencies between 50 Hz and 6.4 kHz according to ISO 10534-2 and ASTM 1050-98 standards.	The nonwoven composite from a cotton and polyester mixture was better than a wool and bicomponent polyester composite in terms of sound absorptivity. Adding acrylic and polypropylene fibers into the mixture improved the absorptivity of sounds with low- to mid-range frequencies. The composite with microfibers was found to perform better in sound absorption due to its low weight and high thickness.
[75]	Poplar wood fiber + Polyester fiber (PET) in 3:1 + Isocyanate adhesive (solid content), resin, foaming agent in 50:6:4.	Sound absorptivity was measured by the impedance tubes method in the frequency range of 50–6400 Hz for every 4 Hz.	The airflow resistivity of the wood fiber/polyester fiber composite up to a certain value was inversely proportional to its sound absorptivity. When the airflow resistivity was further reduced below the optimum value (1.98×10^5 Pa·s/m^2), the value of α decreased. Additionally, the value of α at low frequencies increased with the increase in the cavity width.
[77]	Coir + polyester.	The noise absorption coefficient (NAC) was measured by the reverberation room method, and the transmission loss index was measured as per ISO 717-1.	The coir fiber with a perforated panel had a higher NAC at 500 to 2500 Hz, and beyond that, the coir fiber without a board had a higher coefficient. The coir fiber as a reinforcement in polyester increased the sound absorption coefficient and transmission loss index value of the composite material.
[78]	(Polyol + isocyanate 1:1) + Tea leaf fiber waste	The sound absorptivity of the material was measured at 50 to 6300 Hz; the waves were based on a two-microphone transfer-function method according to ISO 10534-2 and ASTM E1050-98.	Soft foam was found to absorb low- and mid-to-high-range frequencies of sound better than rigid foam; the maximum absorption was found to be at higher frequency ranges. Adding tea leaf fibers into the soft foam increased the sound absorption coefficient by 50%. Adding tea leaf fibers into the rigid form improved its sound-absorbing property in all sound frequencies.
[79]	(Treated rubber/Meranti wood dust) + (Polyol + Isocyanate) polymer foam.	The sound absorption coefficient and the normal specific acoustic impedance ratios of materials as per ASTM E1050 at a frequency range of 100 to 6000 Hz were studied.	The filler loading concentration and particle size in polymer foam influenced the α. The frequency absorption level increased from 2800 Hz to 3700 Hz from light to heavy filler loading composites. The noise reduction coefficient (NRC) was inversely proportional to the wood particle size. The higher the pore size, the lower the NRC.

Table 1. *Cont.*

Ref	Materials	Method	Findings
[80]	Isotactic polypropylene (PP) + lignocellulosic materials derived from hemp, flax, beech, pine, rapeseed straw was used as fillers.	The acoustic standing wave method was applied to determine a material's sound-absorption power at 1000, 1800, 3000, 4000, 5000, and 6300 Hz.	With a hemp filler, the value of the coefficient (α) increased rapidly up to about 25% when the frequency was increased from 3000 to 6300 Hz. For other biofillers, a higher absorptivity was observed at the frequencies of 3000 Hz to 4000 Hz. The inclusion of a biofiller in pure polypropylene increased the absorption of sound above 3000 Hz by about one-fifth.
[81]	Concrete samples: polystyrene granules, polyethylene terephthalate (PET) granules, treated corn cobs, and sunflower stems, and small balls made of sheep wool.	The acoustic absorption was calculated based on the acoustic interferometer technique (Kundt tube). The effect of the thickness was studied.	The sound-absorption coefficients of the composites were considerably higher than the values for conventional concrete. Among the 40 mm samples, the corn-cob composite was the best sound-absorbing material with a noise-reduction coefficient (NRC) of 0.193. For the 80 mm specimens, it was the PET concrete with an NRC of 0.285. The NRC increased by about 1.5 times when doubling the thickness of the sample. Additionally, density and the porosity were the other influencing factors on the sound absorptivity.
[82]	PU (Polyol + isocyanate at 1:1) + Cotton/wool/bamboo (approximately 1 mm long and weight ratios 4%, 8% and 12% for each).	The materials' sound absorptivity was measured as per ISO 10534-2 and ASTM E1050-98 standards.	PU containing 12% cotton fibers resulted in a value of almost 0.8 for sound absorptivity above 2 kHz, which is four times that of pure PU foam. A composition of 4% wool fibers in PU foam offered better sound absorptivity compared to that of virgin PU. PU foam and wool fiber mixed composites result in a maximal sound absorption in most frequencies. Cotton-fiber-blended PU foam absorbs more sound than wool fiber mixed composites. PU containing 4% bamboo fiber foam showed a sound absorptivity of 0.7, which is higher than that of pure PU in the same frequency range. PU with a bamboo fiber absorbed sound more efficiently as compared to the PU with a wool fiber composite. The sound absorptivity was directly proportional to the cotton content in the PU, and indirectly proportional to the bamboo and wool content in the PU.

2.4. Hemp and Biocomposite Materials for Thermal Properties

As the world becomes more inclined towards bio-based materials, it is important to dig deep into the material properties of such biomaterials and specifically, biocomposites. The thermal properties of such materials are becoming of greater interest to help innovate, design, and upgrade the final product and its characteristics to meet various required specifications. The heat behaviour of a material is also useful to understanding its fire properties. There have been several investigations to study the thermal response of various composite materials to determine the factors influencing their thermal conductivities [93–97]. Along with many other factors, the thermal behaviour (thermal conductivity) of a composite material has been found to change with the temperature, quality and quantity of the reinforcement, and the nature, quality, and quantity of the matrix. Meanwhile, the filler material in the matrix in a composite material changes the mechanical properties and has also been found to change the way certain materials behave when heat is applied. One of the most influential properties in the study of the thermal characteristics of composite materials is thermal conductivity, which decides whether the subject under study, when subjected to heat, will either conduct the heat or insulate itself from transmitting heat.

The thermal conductivity (TC) of a material can be determined by applying Fourier's law of heat conduction, which states that the rate of heat transfer through a material is proportional to the negative temperature gradient and the surface area of the material. In polymer composite laminates, heat transfer by conduction is influenced by the type of

plastic used, in addition to its surface area and temperature gradient. Moreover, TC is an anisotropic property [98], which means that the value also depends upon the direction in which it is measured, as shown in Figure 2 below. In Figure 2, T_1 and T_2 are two end temperatures along the x direction of the composite materials with fillers. (T_1 is higher than T_2 so that the heat flows from the left towards the right side.) K_x, K_y, and K_z are the effective thermal conductivities of the resultant material along the z, y, and z directions, respectively. The filler type, shape, orientation, and content are other factors contributing to the change in TC [99]. The TC of semi-crystalline polymers decreases with the increase in the temperature difference from room temperature up to the melting point, due to the increase in specific heat with the rise in temperature. It suddenly rises in the melting zone, reaches the maximum value, and then declines. In amorphous polymers, the thermal conductivity that changes with the temperature depends upon the glass transition temperature, showing two different TC change patterns before the glass transition temperature (rubbery state), and after the glass transition temperature (glassy state) [100].
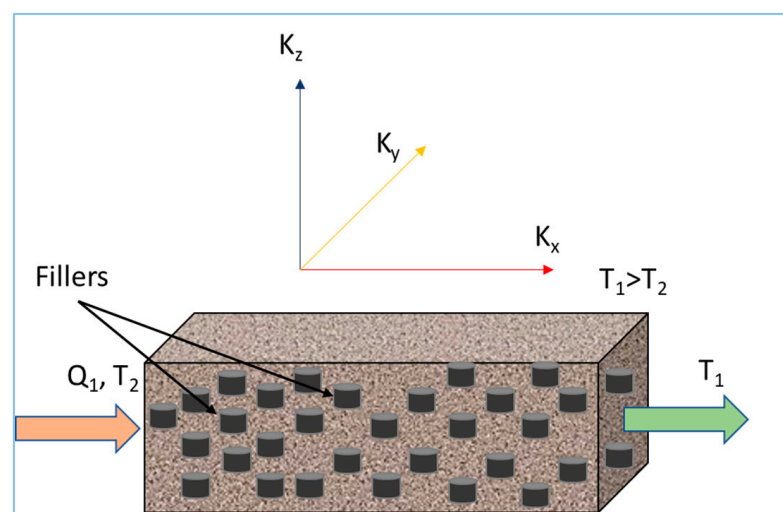
Figure 2. Showing three thermal conductivities as anisotropic properties along x, y, and z directions.

Researchers have been able to determine the thermal conductivity of a material for a long time now. Progressively, the techniques and processes to find the thermal conductivity have changed with the availability of computational tools. In one of these studies, WD Kingery (1955) [93] identified that the presence of oxides (fused silica, Al_2O_3, MgO, BeO) with a higher thermal conductivity causes the normal conductivity and temperature relationship in a material to deviate. This was explained to be the cause of the radiant heat transfer, porosity, emissivity, and electronic conductivity of the specimen. Salgado-Delgado R. et al. (2016) [94] studied the effect of sugarcane charcoal in Portland cement and found that the increased particle loading and increased particle size both reduced the material's thermal conductivity. This has been attributed to the decrease in the contact area with the increase in pore size and air volume due to the increase in the loading and particle size of the filler. Additionally, the presence of oxides in the composite materials also contributed to its reduced thermal conductivity. Pine wood in polyethylene was studied by Bourai K., Riedl B., and Rodrigue D. (2013) [95], and the results showed a compromised thermal conductivity when the wood concentration was increased. The weak bonding between the wood and polyethylene (one hydrophilic and another hydrophobic) interface, resulting in voids and gaps, contributes to this divergence in thermal conductivity (k). Mathematical models have been studied to analyze the thermal properties of the materials. A summary of the findings of the thermal behaviour of various materials is shown below in Table 2.

Table 2. Summary of thermal properties of biofiber-reinforced composites.

Ref.	Materials	Method	Findings
[93]	Single-phase dense ceramics	The approximate wave $-$ velocity was calculated from $v = \sqrt{(E/\rho)}$. The value of k for various oxides calculated based on $k = 1/(8 \, slv)$, where s = heat capacity per unit volume, l = mean path length (calculated as a function of T), and v = wave-velocity. The calculated k for various materials was plotted against 1/T.	Oxides with high thermal conductivity deviated from the usual 1/T relationship at low temperatures below the Debye temperature. The radiant heat transfer caused a rise in the thermal conductivity of metal oxides, such as SiO_2, Al_2O_3, MgO, and BeO, at a high temperature. Similarly, porosity, emissivity, and electronic conductivity are other factors that bring changes to the thermal conductivity with temperature.
[94]	Portland cement (CPC-30R) (4:1 water–cement ratio) and charcoal (CSB) (5%, 10%, and 15% by weight) from sugarcane bagasse.	The thermal conductivities were characterized following ASTM guideline C177 (hot insulated-plate technique).	The thermal conductivity of Portland cement was better than that of the cement–charcoal composite material. CSB content and its particle size demonstrated the effect in the composite material's thermal conductivity. The increased CSB particles in the composite reduced the contact area and increased the pore size and air volume inside the system. From the EDS analysis, it was confirmed that the oxides in the material further contributed to the diminishing thermal conductivity.
[95]	Polyethylene (PE) at 25 °C and 180 °C with pine wood flour up to 20%.	Experimental value of thermal conductivity was calculated with K-System II. Simulations were performed in 2D. The modelled samples were considered to be a binary composite of polymer and reinforcement, contained no voids, and had pores with strong bonding in the matrix and filler interface. MATLAB was used.	The temperature did not affect the thermal conductivity of PE at the solid state. However, the thermal conductivity decreased significantly near its melting point. Again, the temperature did not affect the thermal conductivity of PE at the molten state. On the other hand, the content of the wood filler supressed the thermal conductivity of the resulting material. The difference in the values between the experimental and the simulated models was due to the negligence of the voids in the simulated model, which were present in the experimental samples.
[96]	Powder HDPE with 8% vol. of sand particles (particle size:0.425–0.6 mm). The mixed powder was melted at 185 °C under 4 MPa and was casted into samples, cooled, solidified under pressure, and taken out of the die.	The effective thermal conductivity was measured by the modified hot wire method. k was calculated as: $k = F \cdot Q \cdot \ln(t_2/t_1)/(T_2 - T_1) - H$, (where F is the specific heat constant of the probe, Q is the heat flow per unit of time per unit length heating wire, T_1 and T_2 are temperatures at t_1 s and t_2 s, and H is the specific heat constant of the probe.) The value of k was studied using the Zehner and Schlfinder model, Krupiczka model, and Woodside and Messmer model.	The effect of porosity for granular fillers with $0.35 \leq e \leq 0.6$ on the effective thermal conductivity was accurately predicted by the Zehner and Schlunder model and the Krupiczka model. It was found that increasing the filler grain size increased the effective thermal conductivity of the material. A smaller grain size meant a higher number of grains were required to fill in the same gap, resulting in the heightened thermal resistance.

Moreover, due to their excellent heat-insulating behaviour and light weight, hemp fibers have been consumed and studied for a long time. Hempcrete is the result of using hemp in concrete to reinforce structures and buildings. Researchers have studied its mechanical and thermal properties [97], physical and structural properties [101], its microstructure and its strength [102], the impact of hysteresis and temperature on it [103], its modification to improve its water-repellent behaviour [104], its heat-conducting properties as a wall [105], and its numerical modelling [106]. Various models have been implemented to study hemp composite materials' thermal conductivity. The main matrix in hemp com-

posites is the thermoplastic polymer. The Table 3 below summarizes the analytical studies and their findings in the field of hemp composite materials.

Table 3. Analytical methods to study the thermal conductivity of hemp-based biocomposite materials.

Ref.	Materials	Analytical Method	Findings
[107]	Hemp/PE-PP (9:1) by the carding technique, non-woven samples from the obtained composite webs by thermal bonding.	The two-plate method was used to determine the thermal resistance ($m^2 \cdot K/W$) and the thermal conductivity was measured according to BS 4745:2005.	The thermal conductivity ranged from 0.028 to 0.04 W/(m·K). The value of k depends on the following factors: the thermal resistance of the composite, density, applied temperature, sample moisture content, and porosity.
[108]	Hemp fibers were reinforced with polybutylene terephthalate co-glutarate (PBTG) with three functional additives: i. carbon black, ii. carbon nanotube, and iii. sepiolite.	The thermal resistance of the composite was calculated after measuring the delayed decomposition onset temperature, maximum decomposition temperature, and the residue.	The excellent thermal barrier effect and flame-supressing behaviour of the sepiolite demonstrated a better thermal resistance in the composite sample as compared to those of the other two fillers.
[109]	PU and hemp fiber with fiber-loading ratios of 19:1, 9:1, 17:3, 4:1, 3:1, 7:3.	A thermal conductivity analyser (λ-Meter EP500e) was used to determine the thermal conductivity of the composites. The thermal conductivity measurement consists of applying a variable heat flux in a block which includes a 200 mm × 200 mm × 30 mm sample taken between two plates by ASTM standard ASTMC177.	The PU-hemp fiber composite presented excellent thermal insulating properties. The introduction of hemp fiber into the PU matrix led to an increase in the thermal conductivity as compared to the thermal conductivity of the PU alone.
[110]	Acrylic polymer as well as randomly oriented and aligned hemp fiber were used to prepare the composite.	The transverse and in-plane thermal conductivity of oriented and randomly oriented composites were measured as per the technique proposed by Davidson and James [26]. The thermal conductivity (k) was calculated as $k = J_q \cdot l/T$, where J_q is the measured heat flux crossing the sample, l is the thickness of the sample in the direction of the heat flow, and T is the temperature gradient across the sample. The temperature distribution was found by solving the Fourier heat conduction equation.	The specific heat capacity (C) of fiber from 20 to 100 °C could be represented by: $Cpf = 5 e^{-6} T^2 + 0.0149 T + 1.78$ and for the cured resin: $Cpr = 0.011T + 1.5$. For the composite: $Cpc(T) = Cpf(T) + (1 - vf) Cpr(T)$, where cf = the volume fraction of fiber. The hemp fiber decreased the thermal conductivity (K) value of the composite compared to that of the virgin matrix because of the low value of K for the fiber. The E-S modal and rule of mixture model simulation on the FEM predicted that the transverse K (R^2 0.99) and in-plane oriented/randomly oriented K (R^2 0.95 & 0.92) are in close agreement.
[111]	Manila hemp fiber–polylactic acid (PLA) composites.	A theoretical method was based on Hasselman–Johnson's model. Moreover, the finite element model is applied in 2D to simulate the thermal conductivity of the composite. The model is in a square array suitable for the thermal conduction analysis of fiber composites.	Two different methods produced the same K_{sf} for Manila hemp fiber (about 0.185 W/(m·K)). Although the thermal barrier resistance was neglected, the evaluated value of K_{sf} was valid. These two methods are suitable to calculate the thermal conductivity of any natural fibers. K_{sf} depends on lumen size, but not on the orientation and concentration of the lumen.
[112]	The unsaturated PE resin, Stypol, was chosen as the matrix. A 4 mm mat made of 2:1 hemp fiber and kenaf fiber was chosen as the reinforcement. Another 8 mm thick 100% hemp fiber mat was taken as a reinforcement. A random glass fiber mat was used to prepare a reference composite sample (19% vol. fiber content).	The mould's temperature profile was predicted by a 1-D curing model based on the numerical resolution of the Fourier's heat conduction equation for 1-D transient heat transfer with internal heat generation. The governing equations were integrated by the Crank–Nicholson finite difference method.	The temperature profile obtained from the experiments closely matched the ones predicted from the model within the RTM mould during the curing process.

Table 3. *Cont.*

Ref.	Materials	Analytical Method	Findings
[113]	The numerical model prediction of the clustering effect on the effective thermal conductivity of a hemp-fiber-filled cement composite was performed by developing the N-sided Voronoi fiber/matrix elements.	A fundamental-solution-based hybrid finite element formulation is developed using the FEM (HFS-FEM) with N-sided Voronoi fiber/matrix elements to solve the representative unit cell with defined boundary temperature conditions.	When the number of sides/nodes was increased, the difference between the predicted and theoretical values decreased. The effective thermal conductivity of the composites was not affected by the number of fibers. The increased global volume fraction of the fiber had a diminishing effect on both the clustered as well as well-dispersed fibers in the cement. This was due to the lower thermal conductivity of hemp fiber used in the cement.
[114]	A resin transfer moulding (RTM) process was employed to produce hemp/kenaf fiber-unsaturated PE composites with different fiber contents.	The cure of the resin in the mould was simulated. A 1-D curing model was used. The Crank–Nicholson finite difference method was used to integrate the governing equations.	For the first time, the curing behaviour of such materials was predicted using a curing model based on the resolution of the one-dimensional Fourier's heat conduction equation.

2.5. Hemp Composites for Mechanical Properties

Hemp fibers have been studied for their superior mechanical properties, demonstrated by their high tensile strength and tensile modulus. Shahzad A. (2013) [115], in his study of hemp fiber's physical and mechanical properties, found out the tensile strength was 277 ± 199 MPa, modulus was 9.5 ± 5.8 GPa, and failure strain was 2.3 ± 0.8%. Pickering et al. (2007) [116] found the strengths of hemp fibers with different growing periods. The result showed that the unretted fibers with a 114-day growing period have a tensile strength above 800 MPa. The fibers' mechanical properties were greatly affected by the growing time and the selection between the retted and unretted fibers. The linearly related stress–strain curves for the hemp fibers showed a huge deviation in the tensile properties among the fibers, which is one of the challenges that need to be addressed when compared to uniform synthetic fibers, which offer consistent mechanical properties. On a positive note, these fibers can be used as reinforcements to form strong composite materials. Table 4 summarizes studies on the mechanical properties and water-absorption properties of hemp composite materials.

Table 4. Mechanical properties of hemp-based biocomposite materials.

Ref.	Materials	Procedure	Curing Time	Findings
[117]	Unretted hemp fiber with epoxy resin/hardener (4:1)	A total of 6 cm unretted hemp fiber (volume fraction 0.2) was soaked with epoxy resin/hardener (4:1) for 10 min, and the trapped air was squeezed out. The steel top squeezed out the excess resin.	Forty-eight hours at room temperature, and post curing at 60 °C for an hour.	The novel hemp–epoxy composite showed a Young modulus of 8 GPa and strength of 90 MPa. The pinned hemp fiber (both retted and unretted) showed better tensile strength properties than the tangled standard hemp fibers (both retted and unretted) (Figure 3). The harvest timing was another factor influencing the strength of the fibers, showing a degraded Young's modulus after 90 days of harvest time (Figure 4). The retted fibers showed less variation in their strength properties as compared to the unretted ones, with both offering similar mean strength values.
[118]	Jute, hemp, glassfiber, epoxy (resin 520) and hardener (PAM) (10:1)	The matrix was introduced into 0.3×0.3 m mat by hand layup process at room temperature.	Cured under pressure for 24 h in the mould, and at room temperature for another 12 h.	Hemp/epoxy offered a tensile strength of 75.14 MPa, compression strength of 90.56 MPa, flexural strength of 126.07 MPa, and shear strength of 37.58 MPa. These values are superior compared the jute–epoxy, and jute–hemp–epoxy composites.

Table 4. *Cont.*

Ref.	Materials	Procedure	Curing Time	Findings
[119]	Unidirectional retted hemp fiber, epoxy resin, and its amine hardener (100:28 mass ratio)	Fibers 140 mm long (EDTA/Enzyme/NaOH treated) were vacuum-infused and moulded with the resin to produce 140 mm × 10 mm × 2 mm composites.	NA	The reduction in the pectin in the hemp fibers increased the void spaces, which in turn enhanced the fiber impregnation with epoxy, and resulted in improved mechanical properties (stiffness, strength). The removal of hemicellulose improved the fiber-matrix bond strength and finishing of the fiber surfaces, improved the stiffness of the composites, and decreased the composite's strength.
[120]	Twill woven hemp fabrics, epoxy resin (tetraglycidyl ether of pentaerythritol), and a curing agent (3,3′-dimethyl-4,4′-diamino-dicyclohexyl-methane)	Hemp fiber was treated with H2SO4 (17% by mass) and 5% NH4OH. Another set of fiber was readied by a sol-gel treatment using Geniosil GF-9 amine type silane in a toluene solution (1 g:10 mL). The composites were formed by the hand layup method, keeping two plies of the twill-woven hemp fabric (total thickness 4 mm) and pouring in the epoxy hardener solution.	The composites were cured at room temperature for 24 h, followed by post curing at 80 °C for another 4 h.	The composite with the treated hemp fabric showed a similar tensile strength to that of the untreated fabric composite. An improved elastic modulus, reduced flexural modulus, and reduced flexural strength of the treated fabric composite was seen.
[121]	Pure unbleached plain weave hemp, and epoxy resin (Kinetix R240) with a hardener (H160).	Hemp fabrics with three, four, and six layers (250 mm × 1200 mm) were wetted out with a matrix using the hand layup process.	The composite was vacuumed (approx. 100 kPa) for 15 h at 23 °C.	The unidirectional composites compared to the biaxial woven composites with the same volume of fibers (compared with the literature of Weclawski et al.) showed higher tension strength values (the weave reduced the strength; half of the fiber volume in the woven fabric did not contribute to the unidirectional strength).
[122]	Hemp fiber, and dicyanate ester (CE) of bisphenol-A and bisphenol-A-based benzoxazine (BOZ)	Two kinds of composites were formed with shredded fibers (4 ± 1 mm): one with untreated fibers and resin and another with surface-treated hemp (by the Soxhlet extraction method using ethanol and cyclohexane, mixed in distilled water for 10 h at room temperature, and dried at 60 °C; 0.9 g of silane coupling agent was added in 40 mL of water and 60 mL of ethanol, dried at room temperature for 12 h and vacuum-dried at 50 °C for 12 h) with resin. CE/BOZ resin (90:10 by weight) was heated at 100 °C for 30 min and introduced into an ultrasound bath for 15 min. The fiber was introduced in it and the solution was poured into steel moulds.	The composite was degassed and vacuumed in an oven at 120 °C for 2 h, hydraulically hot-pressed and cured at 180 °C for 2 h, 200 °C for 2 h, and 220 °C for 2 h at 15 MPa.	The flexural strength and flexural modulus of the treated and untreated fiber composites increased with the simultaneous increase in the fiber content. Similarly, the impact strength (explained by the absorbed energy using the Charpy impact during the fracture of the composites) increased with the simultaneous increment of the fibers. The microhardness followed the trend of the flexural properties and impact strength. These properties, with the same percentage composition of the treated fibers, were better than those of the untreated fiber composites.
[123]	Hemp fabric (randomly oriented, non-woven), unsaturated polyester (PE), and methyl ethyl ketone peroxide (0.01 *w/w* of PE)	The hemp fabric was dried at 100 °C, and the matrix was poured into the fabric-containing mould, the composite. A combination of the hand layup and compression moulding methods was employed.	The composite was left for 3 min to release the air bubbles before hydraulically pressing it at 10 bar and 22 °C for 1.5 h. The composite was left to further cure at 22 °C for 24 h, and post-cured at 80 °C for 3 h.	The added layers of fabrics resulted in an elevated water absorption. Moreover, the rate increased when the temperature of the water was increased. The water absorption had no effect on the tensile stress and the stress–strain curve is linear to the point of failure. The flexural stress increased by increasing the fabric layers. The water-absorbed samples showed reduced flexural stress as compared to their properties in the dried state. The tensile and flexural modulus decreased for all wet hemp-reinforced samples as compared to the dry samples.

Table 4. *Cont.*

| Ref.	Materials	Procedure	Curing Time	Findings
[124]	Hemp fiber in four orientations (0°, 90°, 0° and 90°, and 0°, 90°, 45°, and 135°), and methyl ethyl ketone peroxide into vinyl ester (1:44 by wt.)	Fiber resin composites with ten layers with a size of 300 mm × 300 mm were fabricated by the hand layup technique, compressed at 4.36 kPa, left to cure for 24 h in room temperature, and post-cured for 4 h at 80 °C.		Hemp fibers aligned at 0° in the composite based on the warp direction showed the highest tensile strength (68.89 ± 5.51 MPa), lowest tensile strain (2.05 ± 0.12%), and highest tensile modulus of 6.91 (±0.61) GPa. The flexural strength and flexural modulus of the 0° fiber-aligned composite were the greatest, with the values being 109.35 ± 1.96 MPa and 6.31 ± 0.06 GPa, respectively. Also, the impact energy and impact strength of the 0° fiber-aligned composite was the highest. The 90° fiber-aligned composite showed the least tensile, flexural, and impact energy.
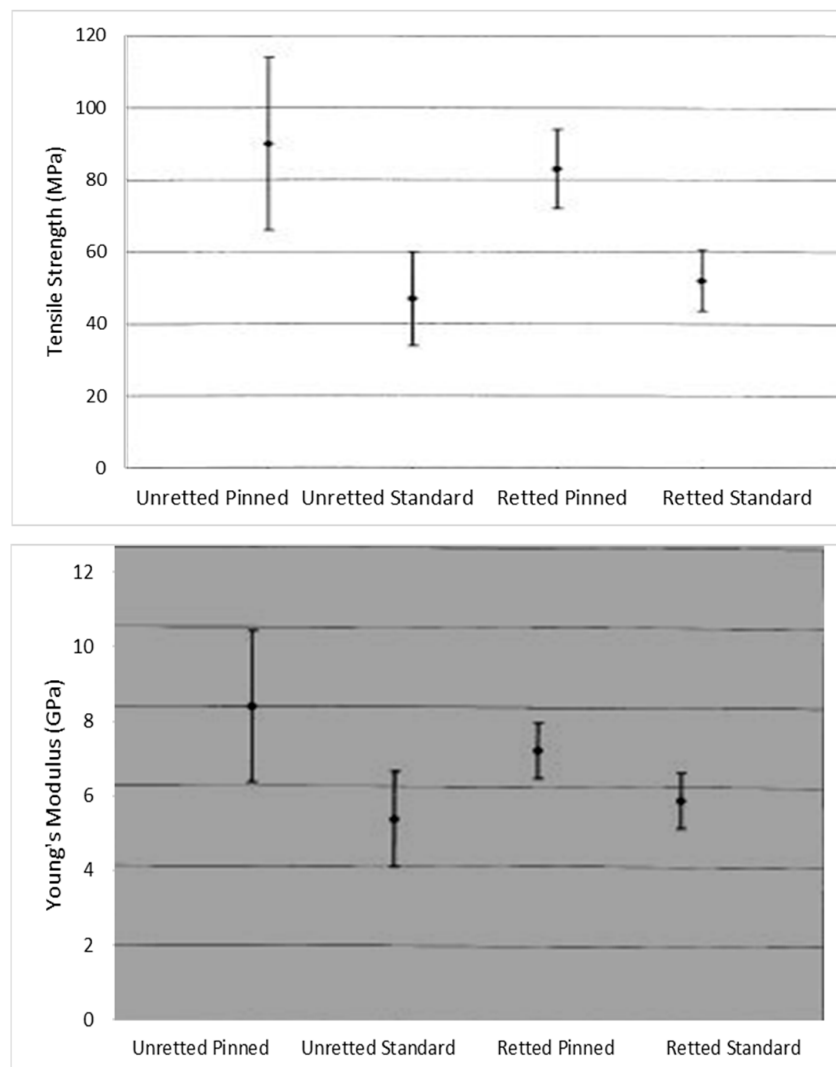
Figure 3. Showing the tensile properties of hemp (retted and unretted)–epoxy composites. Reprinted/adapted with permission from Hepworth DG et al. (2000) [117].
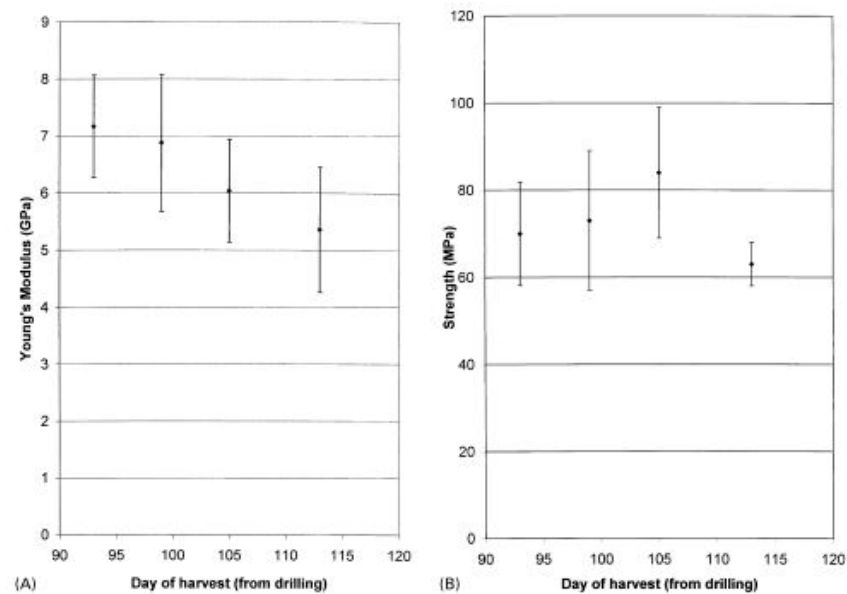
Figure 4. (**A**) Showing the difference in Young's Modulus (in GPa) of hemp fiber against the days of harvest. (**B**) Showing the change in tensile strength (in MPa) as a function of harvest time. Reprinted/adapted with permission from Hepworth DG et al. (2000) [117].

3. Current Issues with Hemp Composite Materials

Apart from the common issues discussed above, lightweight, corrosion-resistant, and mechanically sound hemp composite materials come with cost-related challenges, including recyclability (due to the cross-linked nature of thermostat resin, inorganic fibers, and inorganic fillers). As per the Ford Motor Co. (Dearborn, MI, USA), the substitution of steel, aluminum, and plastic by composites is a challenge due to three main reasons: design optimization, simulations, and assembly [125]. The design optimization process is the most concerning one as it takes longer than that of steel, aluminum, and plastic, because there still are not enough data available on composite materials. The automotive industry has specific time windows for the design and optimization of each part, and while the parts from metal and plastics can be designed and implemented in time, a lack of robust performance data results in an inconvenient and unaffordable design cycle [126].

On the other hand, the extensive consumption of plastics in the present field of composites poses a threat to the environment due to the massive release of volatile gases during their manufacturing processes [126,127]. Once prototyping is conducted, scaleup is another problem when developing composite parts due to the magnification of the effects of numerous variables involved in the production of larger models, which remain dormant in small-sized prototypes and samples. Hemp fiber's texture, shape, surface porosity, and distribution of resin are some of the other factors that can affect composite structures and their performance [126].

Heat is another factor that changes materials' behaviours. For instance, the physical, thermal, and mechanical behaviour of a polymer matrix as well as the hemp fiber in a composite will fluctuate with the exposed temperature/heat. Therefore, it is imperative to study the structural performance and the material's behaviour under thermal and mechanical stress conditions [128]. However, there is not enough information available regarding the physical and mechanical behaviours of hemp composites as a function of temperature. These concerns have led scholars to focus mainly on optimizing the resins and fibers; the empirical manufacturing technologies are still difficult to codify, model, and simulate.

Therefore, aside from the physical and mechanical properties which have been explicitly studied in the composite materials, the thermal effects on these properties and the

development of mathematical models can help optimize hemp fibers' process conditions and hemp composites' manufacturing costs and time.

4. Conclusions

Bio-products from residual wastes will help reduce greenhouse gas emissions by reducing the piling up of wastes in landfills and the environment. The replacement of inorganic fibers, polymers, and inorganic fillers with their bio-based counterparts is the key to ensuring a green and clean environment. The utilization of locally available renewable resources to produce lighter, stronger, more efficient, and economical goods is another aspect of this study.

Based on the literature presented, there is still not enough information to understand the effect of biochar on materials' properties, including sound absorptivity and thermal properties. Studies have suggested that hemp fiber influences the acoustic impedance of a material due to its porous nature. Hemp-based composite materials with and without fillers help us understand the effects of fibers and fillers on materials' behaviours to obtain the optimum proportion of the ingredients and to model materials with analytical studies.

Fundamentally, the utilization of hemp fibers and hemp hurd in polymer composites promotes the bioeconomy by utilizing waste biomass to produce advanced eco-friendly materials. The circular bioeconomy is a concept that will be relevant to any nation willing to advance towards a greener world. The concept of the green economy will generate additional income for farmers, create local-level jobs, and clean up our surroundings by reducing our carbon footprint. As a result, this will have a positive impact on society, the economy and the environment, the three pillars of sustainability. The utilization of under-utilized hemp waste will help greatly to manage agricultural waste.

Author Contributions: Conceptualization, R.K.D.; methodology, R.K.D.; validation, B.A. and A.D.; formal analysis, R.K.D.; investigation, R.K.D.; resources, B.A. and A.D.; data curation, B.A.; writing—original draft preparation, R.K.D.; writing—review and editing, R.K.D.; supervision, B.A. and A.D.; project administration, A.D.; funding acquisition, A.D. All authors have read and agreed to the published version of the manuscript.

Institutional Review Board Statement: Not Applicable.

Informed Consent Statement: Not Applicable.

Conflicts of Interest: The authors declare no conflict of interest.

References

1. Šerifi, V.; Tarić, M.; Jevtić, D.; Ristovski, A.; Isović, M.Š. Historical Development of Composite Materials. *Ann. Oradea Univ. Fascicle Manag. Technol. Eng.* **2018**, *25*, 2018-3. [CrossRef]
2. Jamison, R.; Griffin, O.; Ecker, J.; Skullney, W. Use of Graphite/Epoxy Composites in Spacecraft Structures: A Case Study. *Johns Hopkins APL Tech. Digest.* **1986**, *7*, 3.
3. Varvani-Farahani, A. Composite Materials: Characterization, Fabrication and Application-Research Challenges and Directions. *Appl. Compos. Mater.* **2010**, *17*, 63–67. [CrossRef]
4. Brasington, A.; Sacco, C.; Halbritter, J.; Wehbe, R.; Harik, R. Automated fiber placement: A review of history, current technologies, and future paths forward. *Compos. Part C Open Access* **2021**, *6*, 100182. [CrossRef]
5. Canada to host the 2020 World Circular Economy Forum. *Environ. Clim. Chang. Canada*. Available online: https://www.canada.ca/en/environment-climate-change/news/2019/06/canada-to-host-the-2020-world-circular-economy-forum.html (accessed on 9 September 2021).
6. Hill, C.A.S.; Norton, A.; Newman, G. The water vapor sorption behavior of natural fibers. *J. Appl. Polym. Sci.* **2009**, *112*, 1524–1537. [CrossRef]
7. Madsen, B.; Brøndsted, P.; Andersen, T.L. Biobased composites: Materials, properties and potential applications as wind turbine blade materials. In *Advances in Wind Turbine Blade Design and Materials*; Elsevier: Amsterdam, The Netherlands, 2013; pp. 363–386.
8. Babu, R.P.; Oconnor, K.; Seeram, R. Current progress on bio-based polymers and their future trends. *Prog. Biomater.* **2013**, *2*, 8. [CrossRef]

9. Dawande, R. Bioplastics Market Overview. Available online: https://www.alliedmarketresearch.com/bioplastics-market (accessed on 9 September 2021).

10. Bharath, K.N.; Basavarajappa, S. Applications of biocomposite materials based on natural fibers from renewable resources: A review. *Sci. Eng. Compos. Mater.* **2016**, *23*, 123–133. [CrossRef]

11. Sun, W.; Lipka, S.M.; Swartz, C.; Williams, D.; Yang, F. Hemp-derived activated carbons for supercapacitors. *Carbon N. Y.* **2016**, *103*, 181–192. [CrossRef]

12. Giorcelli, M.; Bartoli, M. Development of Coffee Biochar Filler for the Production of Electrical Conductive Reinforced Plastic. *Polymers* **2019**, *11*, 1916. [CrossRef]

13. Nan, N.; DeVallance, D.B.; Xie, X.; Wang, J. The effect of bio-carbon addition on the electrical, mechanical, and thermal properties of polyvinyl alcohol/biochar composites. *J. Compos. Mater.* **2016**, *50*, 1161–1168. [CrossRef]

14. Chandramohan, D.; Presin Kumar, A.J. Experimental data on the properties of natural fiber particle reinforced polymer composite material. *Data Brief* **2017**, *13*, 460–468. [CrossRef]

15. Abdellatef, Y.; Khan, M.A.; Khan, A.; Alam, M.I.; Kavgic, M. Mechanical, Thermal, and Moisture Buffering Properties of Novel Insulating Hemp-Lime Composite Building Materials. *Materials* **2020**, *13*, 5000. [CrossRef] [PubMed]

16. Zouari, M.; Devallance, D.B.; Marrot, L. Effect of Biochar Addition on Mechanical Properties, Thermal Stability, and Water Resistance of Hemp-Polylactic Acid (PLA) Composites. *Materials* **2022**, *15*, 2271. [CrossRef]

17. Dev, S.; Aherwar, A.; Patnaik, A. Preliminary Evaluations on Development of Recycled Porcelain Reinforced LM-26/Al-Si10Cu3Mg1 Alloy for Piston Materials. *Silicon* **2019**, *11*, 1557–1573. [CrossRef]

18. Surappa, M.K. Aluminium matrix composites: Challenges and opportunities. *Sadhana* **2003**, *28*, 319–334. [CrossRef]

19. Sharma, A.K.; Bhandari, R.; Aherwar, A.; Rimašauskienė, R. Matrix materials used in composites: A comprehensive study. *Mater. Today Proc.* **2020**, *21*, 1559–1562. [CrossRef]

20. Doddi, P.R.V.; Chanamala, R.; Dora, S.P. Effect of fiber orientation on dynamic mechanical properties of PALF hybridized with basalt reinforced epoxy composites. *Mater. Res. Express* **2020**, *7*, 015329. [CrossRef]

21. Yong, C.K.; Ching, Y.C.; Chuah, C.H.; Liou, N.-S. Effect of Fiber Orientation on Mechanical Properties of Kenaf-Reinforced Polymer Composite. *BioResources* **2015**, *10*, 2597–2608. [CrossRef]

22. Alomayri, T.; Shaikh, F.U.A.; Low, I.M. Effect of fabric orientation on mechanical properties of cotton fabric reinforced geopolymer composites. *Mater. Des.* **2014**, *57*, 360–365. [CrossRef]

23. Zhang, H.; Huang, Y.; Lin, M.; Yang, Z. Effects of fibre orientation on tensile properties of ultra high performance fibre reinforced concrete based on meso-scale Monte Carlo simulations. *Compos. Struct.* **2022**, *287*, 115331. [CrossRef]

24. Ramakrishnan, T.; Sathesh, B.M.; Balasubramani, S.; Manickaraj, K.; Jeyakumar, R. Effect of Fiber Orientation and Mechanical Properties of Natural Fiber Reinforced Polymer Composites—A Review. *Paid. J. Res.* **2021**, *14*, 17–23.

25. Cordin, M.; Bechtold, T.; Pham, T. Effect of fibre orientation on the mechanical properties of polypropylene–lyocell composites. *Cellulose* **2018**, *25*, 7197–7210. [CrossRef]

26. McCardle, R.; Bhattacharyya, D.; Fakirov, S. Effect of Reinforcement Orientation on the Mechanical Properties of Microfibrillar PP/PET and PET Single-Polymer Composites. *Macromol. Mater. Eng.* **2012**, *297*, 711–723. [CrossRef]

27. Vinayagamoorthy, R. Effect of particle sizes on the mechanical behaviour of limestone-reinforced hybrid plastics. *Polym. Polym. Compos.* **2020**, *28*, 410–420. [CrossRef]

28. Youssef, Y.; El-Sayed, M. Effect of Reinforcement Particle Size and Weight Fraction on the Mechanical Properties of SiC Particle Reinforced Al Metal Matrix Composites. *Int. Rev. Mech. Eng.* **2016**, *10*, 261. [CrossRef]

29. Yang, Z.; Fan, J.; Liu, Y.; Nie, J.; Yang, Z.; Kang, Y. Effect of the Particle Size and Matrix Strength on Strengthening and Damage Process of the Particle Reinforced Metal Matrix Composites. *Materials* **2021**, *14*, 675. [CrossRef]

30. Saba, F.; Zhang, F.; Liu, S.; Liu, T. Reinforcement size dependence of mechanical properties and strengthening mechanisms in diamond reinforced titanium metal matrix composites. *Compos. Part B Eng.* **2019**, *167*, 7–19. [CrossRef]

31. Paknia, A.; Pramanik, A.; Dixit, A.R.; Chattopadhyaya, S. Effect of Size, Content and Shape of Reinforcements on the Behavior of Metal Matrix Composites (MMCs) Under Tension. *J. Mater. Eng. Perform.* **2016**, *25*, 4444–4459. [CrossRef]

32. Gong, Y.; Niu, P.; Wang, X.; Long, S.; Yang, J. Influence of processing temperatures on fiber dimensions and microstructure of polypropylene/hemp fiber composites. *J. Reinf. Plast. Compos.* **2012**, *31*, 1282–1290. [CrossRef]

33. Manaia, J.P.; Manaia, A.T.; Rodriges, L. Industrial Hemp Fibers: An Overview. *Fibers* **2019**, *7*, 106. [CrossRef]

34. Ngaowthong, C.; Rungsardthong, V.; Siengchin, S. Polypropylene/hemp woody core fiber composites: Morphology, mechanical, thermal properties, and water absorption behaviors. *Adv. Mech. Eng.* **2016**, *8*, 168781401663831. [CrossRef]

35. Sullins, T.; Pillay, S.; Komus, A.; Ning, H. Hemp fiber reinforced polypropylene composites: The effects of material treatments. *Compos. Part B Eng.* **2017**, *114*, 15–22. [CrossRef]

36. Peltola, H.; Madsen, B.; Joffe, R.; Nättinen, K. Experimental Study of Fiber Length and Orientation in Injection Molded Natural Fiber/Starch Acetate Composites. *Adv. Mater. Sci. Eng.* **2011**, *2011*, 891940. [CrossRef]

37. Dupuis, A.; Pesce, J.-J.; Ferreira, P.; Régnier, G. Fiber Orientation and Concentration in an Injection-Molded Ethylene-Propylene Copolymer Reinforced by Hemp. *Polymers* **2020**, *12*, 2771. [CrossRef] [PubMed]

38. Ferreira, R.T.L.; Ashcroft, I.A. Optimal orientation of fibre composites for strength based on Hashin's criteria optimality conditions. *Struct. Multidiscip. Optim.* **2020**, *61*, 2155–2176. [CrossRef]

39. Heitkamp, T.; Kuschmitz, S.; Girnth, S.; Marx, J.-D.; Klawitter, G.; Waldt, N.; Vietor, T. Stress-adapted fiber orientation along the principal stress directions for continuous fiber-reinforced material extrusion. *Prog. Addit. Manuf.* **2022**. [CrossRef]

40. Sharba, M.J.; Leman, Z.; Sultan, M.T.H. Fatigue life prediction of textile/woven hybrid composites. In *Durability and Life Prediction in Biocomposites, Fibre-Reinforced Composites and Hybrid Composites*; Elsevier: Amsterdam, The Netherlands, 2019; pp. 63–82.

41. Hoa, S.V. 2.1 Manufacturing of Composites—An Overview. In *Comprehensive Composite Materials II*; Elsevier: Amsterdam, The Netherlands, 2018; pp. 1–23.

42. Anand, P.B.; Lakshmikanthan, A.; Gowdru Chandrashekarappa, M.P.; Selvan, C.P.; Pimenov, D.Y.; Giasin, K. Experimental Investigation of Effect of Fiber Length on Mechanical, Wear, and Morphological Behavior of Silane-Treated Pineapple Leaf Fiber Reinforced Polymer Composites. *Fibers* **2022**, *10*, 56. [CrossRef]

43. Zhang, P.; Yang, Y.; Wang, J.; Jiao, M.; Ling, Y. Fracture Models and Effect of Fibers on Fracture Properties of Cementitious Composites—A Review. *Materials* **2020**, *13*, 5495. [CrossRef]

44. Callister, W.D.; Rethwisch, D.G. Composites. In *Materials Science and Engineering: An Introduction*; Wiley-VCH Verlag GmbH & Co. KGaA: Weinheim, Germany, 2013; pp. 577–617. ISBN 9781118546895/111854689X.

45. Mohonee, V.K.; Goh, K.L. Effects of fibre–fibre interaction on stress uptake in discontinuous fibre reinforced composites. *Compos. Part B Eng.* **2016**, *86*, 221–228. [CrossRef]

46. Taliercio, A. Generalized plane strain finite element model for the analysis of elastoplastic composites. *Int. J. Solids Struct.* **2005**, *42*, 2361–2379. [CrossRef]

47. Mondali, M.; Abedian, A.; Ghavami, A. A new analytical shear-lag based model for prediction of the steady state creep deformations of some short fiber composites. *Mater. Des.* **2009**, *30*, 1075–1084. [CrossRef]

48. Hu, Y.-G.; Ma, Y.L.; Hu, C.P.; Lu, X.Y.; Gu, S.T. Analysis of stress transfer in short fiber-reinforced composites with a partial damage interface by a shear-lag model. *Mech. Mater.* **2021**, *160*, 103966. [CrossRef]

49. Veer Singh, C. 2.7 Micromechanics of Damage Evolution in Laminates. In *Comprehensive Composite Materials II*; Elsevier: Amsterdam, The Netherlands, 2018; pp. 118–147.

50. van de Werken, N. *Effect of Alignment, Sizing, and Manufacturing Method on Mechanical Properties of Recycled Carbon Fiber Composites*; University of New Mexico: Albuquerque, NM, USA, 2017.

51. Ivey, M.; Melenka, G.W.; Carey, J.P.; Ayranci, C. Characterizing short-fiber-reinforced composites produced using additive manufacturing. *Adv. Manuf. Polym. Compos. Sci.* **2017**, *3*, 81–91. [CrossRef]

52. Chou, T.-W. Short-fiber composites. In *Microstructural Design of Fiber Composites*; Cambridge University Press: Cambridge, UK, 1992; pp. 169–230.

53. Mandell, J.F. Fatigue Behavior of Short Fiber Composite Materials. *Compos. Mater. Ser.* **1991**, *4*, 231–337.

54. Monfared, V. Problems in short-fiber composites and analysis of chopped fiber-reinforced materials. In *New Materials in Civil Engineering*; Elsevier: Amsterdam, The Netherlands, 2020; pp. 919–1043.

55. Mallick, P.K. Thermoplastics and thermoplastic–matrix composites for lightweight automotive structures. In *Materials, Design and Manufacturing for Lightweight Vehicles*; Elsevier: Amsterdam, The Netherlands, 2021; pp. 187–228.

56. Sałasińska, K.; Cabulis, P.; Kirpluks, M.; Kovalovs, A.; Kozikowski, P.; Barczewski, M.; Celiński, M.; Mizera, K.; Gałecka, M.; Skukis, E.; et al. The Effect of Manufacture Process on Mechanical Properties and Burning Behavior of Epoxy-Based Hybrid Composites. *Materials* **2022**, *15*, 301. [CrossRef] [PubMed]

57. Ujianto, O.; Nugroho, A.; Setijotomo, H.S.; Bintoro, A. Effect of Fabrication Techniques, Resin Types and Fiber Combinations on Mechanical Properties and Morphology of Glass Fiber Composites. *Int. J. Mater. Mech. Manuf.* **2020**, *8*, 17–21. [CrossRef]

58. Kim, D.; Hennigan, D.J.; Beavers, K.D. Effect of fabrication processes on mechanical properties of glass fiber reinforced polymer composites for 49 meter (160 foot) recreational yachts. *Int. J. Nav. Arch. Ocean Eng.* **2010**, *2*, 45–56. [CrossRef]

59. Gollins, K. *Comparison of Manufacturing Techniques for Composites Subjected to High Speed Impact*; City University of New York: New York City, NY, USA, 2014.

60. Gholampour, A.; Ozbakkaloglu, T. A review of natural fiber composites: Properties, modification and processing techniques, characterization, applications. *J. Mater. Sci.* **2020**, *55*, 829–892. [CrossRef]

61. Khan, L.A.; Mehmood, A.H. Cost-effective composites manufacturing processes for automotive applications. In *Lightweight Composite Structures in Transport*; Elsevier: Amsterdam, The Netherlands, 2016; pp. 93–119.

62. Xu, W.; Zhang, L. Tool wear and its effect on the surface integrity in the machining of fibre-reinforced polymer composites. *Compos. Struct.* **2018**, *188*, 257–265. [CrossRef]

63. Sheikh-Ahmad, J.; Davim, J.P. Tool wear in machining processes for composites. In *Machining Technology for Composite Materials*; Elsevier: Amsterdam, The Netherlands, 2012; pp. 116–153.

64. Goettler, C.M. *Effect of Density on Friction and Wear Performance of Carbon-Carbon Composite Materials*; Southern Illinois University: Carbondale, IL, USA, 2020.

65. Rahimian, M.; Parvin, N.; Ehsani, N. The effect of production parameters on microstructure and wear resistance of powder metallurgy Al–Al$_2$O$_3$ composite. *Mater. Des.* **2011**, *32*, 1031–1038. [CrossRef]

66. Guell, D.; Bénard, A. Flow-induced alignment in composite materials: Current applications and future prospects. In *Flow-Induced Alignment in Composite Materials*; Elsevier: Amsterdam, The Netherlands, 1997; pp. 1–42.

67. Sakthivel, S.; Senthil Kumar, S.; Solomon, E.; Getahun, G.; Admassu, Y.; Bogale, M.; Gedilu, M.; Aduna, A.; Abedom, F. Sound absorbing and insulating properties of natural fiber hybrid composites using sugarcane bagasse and bamboo charcoal. *J. Eng. Fibers Fabr.* **2021**, *16*, 155892502110448. [CrossRef]

68. Mati-Baouche, N.; de Baynast, H.; Michaud, P.; Dupont, T.; Leclaire, P. Sound absorption properties of a sunflower composite made from crushed stem particles and from chitosan bio-binder. *Appl. Acoust.* **2016**, *111*, 179–187. [CrossRef]

69. Guo, J. *Investigating Acoustic Properties of Biocomposite from Waste Streams*; University of Regina: Regina, SK, Canada, 2016.

70. Koruk, H.; Genc, G. Acoustic and mechanical properties of luffa fiber-reinforced biocomposites. In *Mechanical and Physical Testing of Biocomposites, Fibre-Reinforced Composites and Hybrid Composites*; Elsevier: Amsterdam, The Netherlands, 2019; pp. 325–341.

71. Yao, R.; Yao, Z.; Zhou, J.; Liu, P. Mechanical and acoustical properties of polylactic acid based multilayer-structured foam biocomposites. *J. Reinf. Plast. Compos.* **2016**, *35*, 785–795. [CrossRef]

72. Ghaffari Mosanenzadeh, S.; Naguib, H.E.; Park, C.B.; Atalla, N. Effect of biopolymer blends on physical and Acoustical properties of biocomposite foams. *J. Polym. Sci. Part B Polym. Phys.* **2014**, *52*, 1002–1013. [CrossRef]

73. Liu, D.; Xia, K.; Yang, R.; Li, J.; Chen, K.; Nazhad, M. Manufacturing of a biocomposite with both thermal and acoustic properties. *J. Compos. Mater.* **2012**, *46*, 1011–1020. [CrossRef]

74. Küçük, M.; Korkmaz, Y. The effect of physical parameters on sound absorption properties of natural fiber mixed nonwoven composites. *Text. Res. J.* **2012**, *82*, 2043–2053. [CrossRef]

75. Peng, L.; Song, B.; Wang, J.; Wang, D. Mechanic and Acoustic Properties of the Sound-Absorbing Material Made from Natural Fiber and Polyester. *Adv. Mater. Sci. Eng.* **2015**, *2015*, 274913. [CrossRef]

76. Gayathri, R.; Vasanthakumari, R.; Padmanabhan, C. Sound absorption, Thermal and Mechanical behavior of Polyurethane foam modified with Nano silica, Nano clay and Crumb rubber fillers. *Int. J. Sci. Eng. Res.* **2013**, *4*, 301–308.

77. Zulkifli, R.; Nor, M.J.M.; Tahir, M.F.M.; Ismail, A.R.; Nuawi, M.Z. Acoustic Properties of Multi-Layer Coir Fibres Sound Absorption Panel. *J. Appl. Sci.* **2008**, *8*, 3709–3714. [CrossRef]

78. Çelebi, S.; Küçük, H. Acoustic Properties of Tea-Leaf Fiber Mixed Polyurethane Composites. *Cell. Polym.* **2012**, *31*, 241–256. [CrossRef]

79. Sa'Adon, S.; Rus, A.Z.M. Acoustical Behavior of Treated Wood Dust-Filler for Polymer Foam Composite. *Appl. Mech. Mater.* **2013**, *465–466*, 1039–1043. [CrossRef]

80. Markiewicz, E.; Paukszta, D.; Borysiak, S. *Polypropylene*; Dogan, F., Ed.; InTech: London, UK, 2012; p. 193.

81. Oancea, I.; Bujoreanu, C.; Budescu, M.; Benchea, M.; Grădinaru, C.M. Considerations on sound absorption coefficient of sustainable concrete with different waste replacements. *J. Clean. Prod.* **2018**, *203*, 301–312. [CrossRef]

82. Büyükakinci, B.; Sökmen, N.; Küçük, H. Thermal conductivity and acoustic properties of natural fiber mixed polyurethane composites. *Tekst. Konfeksiyon* **2011**, *21*, 124–132.

83. Hui, Z.; Fan, X. Sound Absorption Properties of Hemp Fibrous Assembly Absorbers. *Seni Gakkaishi* **2009**, *65*, 191–196. [CrossRef]

84. Buksnowitz, C.; Adusumalli, R.; Pahler, A.; Sixta, H.; Gindl, W. Acoustical properties of Lyocell, hemp, and flax composites. *J. Reinf. Plast. Compos.* **2010**, *29*, 3149–3154. [CrossRef]

85. Mehdi Jalili, M.; Yahya Mousavi, S.; Pirayeshfar, A.S. Investigating the acoustical properties of carbon fiber-, glass fiber-, and hemp fiber-reinforced polyester composites. *Polym. Compos.* **2014**, *35*, 2103–2111. [CrossRef]

86. Glé, P.; Gourdon, E.; Arnaud, L. Modelling of the acoustical properties of hemp particles. *Constr. Build. Mater.* **2012**, *37*, 801–811. [CrossRef]

87. Bütschi, P.-Y.; Deschenaux, C.; Miao, B.; Srivastava, N.K. Caractérisation d'une maçonnerie composée d'éléments en aggloméré de chanvre. *Can. J. Civ. Eng.* **2004**, *31*, 526–529. [CrossRef]

88. Degrave-Lemeurs, M.; Glé, P.; Hellouin de Menibus, A. Acoustical properties of hemp concretes for buildings thermal insulation: Application to clay and lime binders. *Constr. Build. Mater.* **2018**, *160*, 462–474. [CrossRef]

89. Fernea, R.; Manea, D.L.; Plesa, L.; Iernuțan, R.; Dumitran, M. Acoustic and thermal properties of hemp-cement building materials. *Procedia Manuf.* **2019**, *32*, 208–215. [CrossRef]

90. Oral, I. Determination of elastic constants of epoxy resin/biochar composites by ultrasonic pulse echo overlap method. *Polym. Compos.* **2016**, *37*, 2907–2915. [CrossRef]

91. Coates, M.; Kierzkowski, M. Acoustic Textiles—Lighter, thinner and more absorbent. *Tech.-Text.-Int.* **2002**.

92. Cuthbertson, D.; Berardi, U.; Briens, C.; Berruti, F. Biochar from residual biomass as a concrete filler for improved thermal and acoustic properties. *Biomass-Bioenergy* **2019**, *120*, 77–83. [CrossRef]

93. Kingery, W.D. Thermal Conductivity: XII, Temperature Dependence of Conductivity for Single-Phase Ceramics. *J. Am. Ceram. Soc.* **1955**, *38*, 251–255. [CrossRef]

94. Salgado-Delgado, R.; Olarte-Paredes, A.; Salgado-Delgado, A.M.; Vargas-Galarza, Z.; Lopez-Lara, T.; Hernández-Zaragoza, J.B.; Rico-Rodríguez, I.; Martínez-Barrera, G. An Analysis of the Thermal Conductivity of Composite Materials (CPC-30R/Charcoal from Sugarcane Bagasse) Using the Hot Insulated Plate Technique. *Adv. Mater. Sci. Eng.* **2016**, *2016*, 4950576. [CrossRef]

95. Bourai, K.; Riedl, B.; Rodrigue, D. Effect of Temperature on the Thermal Conductivity of Wood-Plastic Composites. *Polym. Polym. Compos.* **2013**, *21*, 413–422. [CrossRef]

96. Tavman, I.H. Effective thermal conductivity of granular porous materials. *Int. Commun. Heat Mass Transf.* **1996**, *23*, 169–176. [CrossRef]

97. Parcesepe, E.; De Masi, R.F.; Lima, C.; Mauro, G.M.; Pecce, M.R.; Maddaloni, G. Assessment of Mechanical and Thermal Properties of Hemp-Lime Mortar. *Materials* **2021**, *14*, 882. [CrossRef]

98. Amiri Delouei, A.; Emamian, A.; Sajjadi, H.; Atashafrooz, M.; Li, Y.; Wang, L.-P.; Jing, D.; Xie, G. A Comprehensive Review on Multi-Dimensional Heat Conduction of Multi-Layer and Composite Structures: Analytical Solutions. *J. Therm. Sci.* **2021**, *30*, 1875–1907. [CrossRef]

99. Wieme, T.; Tang, D.; Delva, L.; D'Hooge, D.R.; Cardon, L. The relevance of material and processing parameters on the thermal conductivity of thermoplastic composites. *Polym. Eng. Sci.* **2018**, *58*, 466–474. [CrossRef]

100. Dos Santos, W.N.; de Sousa, J.A.; Gregorio, R. Thermal conductivity behaviour of polymers around glass transition and crystalline melting temperatures. *Polym. Test.* **2013**, *32*, 987–994. [CrossRef]

101. Balčiūnas, G.; Vėjelis, S.; Vaitkus, S.; Kairytė, A. Physical Properties and Structure of Composite Made by Using Hemp Hurds and Different Binding Materials. *Procedia Eng.* **2013**, *57*, 159–166. [CrossRef]

102. Jothilingam, M.; Paul, P. Study on strength and microstructure of hempcrete. In Proceedings of the 7th National Conference on Hierarchically Structured Materials (NCHSM 2019), Chennai, India, 22–23 February 2019; AIP Publishing LLC: Melville, NY, USA; 2117, p. 020028. [CrossRef]

103. Costantine, G.; Maalouf, C.; Moussa, T.; Kinab, E.; Polidori, G. Hygrothermal evaluation of hemp concrete at wall and room scales: Impact of hysteresis and temperature dependency of sorption curves. *J. Build. Phys.* **2020**, *44*, 183–224. [CrossRef]

104. Hussain, A.; Calabria-Holley, J.; Jiang, Y.; Lawrence, M. Modification of hemp shiv properties using water-repellent sol–gel coatings. *J. Sol-Gel Sci. Technol.* **2018**, *86*, 187–197. [CrossRef] [PubMed]

105. Pochwała, S.; Makiola, D.; Anweiler, S.; Böhm, M. The Heat Conductivity Properties of Hemp–Lime Composite Material Used in Single-Family Buildings. *Materials* **2020**, *13*, 1011. [CrossRef]

106. Costantine, G.; Maalouf, C.; Moussa, T.; Polidori, G.; Kinab, E. Numerical modelling of a hemp concrete wall. *E3S Web Conf.* **2019**, *85*, 08003. [CrossRef]

107. Freivalde, L.; Kukle, S.; Russell, S. Thermal properties of hemp fibre non-woven materials. *IOP Conf. Ser. Mater. Sci. Eng.* **2013**, *49*, 012030. [CrossRef]

108. Park, Y.S.; Joo, C.W. Effects of nanoparticles on tensile, electrical, and thermal properties of Hemp/PBTG composites. *Fibers Polym.* **2016**, *17*, 1934–1944. [CrossRef]

109. Sair, S.; Oushabi, A.; Kammouni, A.; Tanane, O.; Abboud, Y.; El Bouari, A. Mechanical and thermal conductivity properties of hemp fiber reinforced polyurethane composites. *Case Stud. Constr. Mater.* **2018**, *8*, 203–212. [CrossRef]

110. Behzad, T.; Sain, M. Measurement and prediction of thermal conductivity for hemp fiber reinforced composites. *Polym. Eng. Sci.* **2007**, *47*, 977–983. [CrossRef]

111. Liu, K.; Takagi, H.; Yang, Z. Evaluation of transverse thermal conductivity of Manila hemp fiber in solid region using theoretical method and finite element method. *Mater. Des.* **2011**, *32*, 4586–4589. [CrossRef]

112. Rouison, D.; Sain, M.; Couturier, M. Resin transfer molding of natural fiber reinforced composites: Cure simulation. *Compos. Sci. Technol.* **2004**, *64*, 629–644. [CrossRef]

113. Progelhof, R.C.; Throne, J.L.; Ruetsch, R.R. Methods for predicting the thermal conductivity of composite systems: A review. *Polym. Eng. Sci.* **1976**, *16*, 615–625. [CrossRef]

114. Behrens, E. Thermal Conductivities of Composite Materials. *J. Compos. Mater.* **1968**, *2*, 2–17. [CrossRef]

115. Shahzad, A. A Study in Physical and Mechanical Properties of Hemp Fibres. *Adv. Mater. Sci. Eng.* **2013**, *2013*, 325085. [CrossRef]

116. Pickering, K.L.; Beckermann, G.W.; Alam, S.N.; Foreman, N.J. Optimising industrial hemp fibre for composites. *Compos. Part A Appl. Sci. Manuf.* **2007**, *38*, 461–468. [CrossRef]

117. Hepworth, D.; Hobson, R.; Bruce, D.; Farrent, J. The use of unretted hemp fibre in composite manufacture. *Compos. Part A Appl. Sci. Manuf.* **2000**, *31*, 1279–1283. [CrossRef]

118. Sature, P.; Mache, A. Mechanical Characterization and Water Absorption Studies on Jute/Hemp Reinforced Hybrid Composites. *Am. J. Mater. Sci.* **2015**, *5*, 129–133. [CrossRef]

119. Liu, M.; Meyer, A.S.; Fernando, D.; Silva, D.A.S.; Daniel, G.; Thygesen, A. Effect of pectin and hemicellulose removal from hemp fibres on the mechanical properties of unidirectional hemp/epoxy composites. *Compos. Part A Appl. Sci. Manuf.* **2016**, *90*, 724–735. [CrossRef]

120. Szolnoki, B.; Bocz, K.; Sóti, P.L.; Bodzay, B.; Zimonyi, E.; Toldy, A.; Morlin, B.; Bujnowicz, K.; Wladyka-Przybylak, M.; Marosi, G. Development of natural fibre reinforced flame retarded epoxy resin composites. *Polym. Degrad. Stab.* **2015**, *119*, 68–76. [CrossRef]

121. Bambach, M.R. Compression strength of natural fibre composite plates and sections of flax, jute and hemp. *Thin-Walled Struct.* **2017**, *119*, 103–113. [CrossRef]

122. Zegaoui, A.; Ma, R.; Dayo, A.Q.; Derradji, M.; Wang, J.; Liu, W.; Xu, Y.; Cai, W. Morphological, mechanical and thermal properties of cyanate ester/benzoxazine resin composites reinforced by silane treated natural hemp fibers. *Chin. J. Chem. Eng.* **2018**, *26*, 1219–1228. [CrossRef]

123. Dhakal, H.; Zhang, Z.; Richardson, M. Effect of water absorption on the mechanical properties of hemp fibre reinforced unsaturated polyester composites. *Compos. Sci. Technol.* **2007**, *67*, 1674–1683. [CrossRef]

124. Misnon, I.; Islam, M.; Epaarachchi, J.; Lau, K.; Wang, H. Fabric Parameter Effect on the Mechanical Properties of Woven Hemp Fabric Reinforced Composites as an Alternative to Wood Products. *Adv. Res. Text. Eng.* **2016**, *1*, 1004.

125. Sloan, J. Composites W. Available online: https://www.compositesworld.com/articles/biggest-hurdles-for-automotive-composites- (accessed on 25 June 2020).

126. Griffin, D.A.; Ashwill, T.D. Alternative Composite Materials for Megawatt-Scale Wind Turbine Blades: Design Considerations and Recommended Testing. *J. Sol. Energy Eng.* **2003**, *125*, 515–521. [CrossRef]

127. Ribeiro, M.; Dinis, M. On the Recyclability of Glass Fiber Reinforced Thermoset Polymeric Composites towards the Sustainability of Polymers' Industry. *Int. J. Waste Resour.* **2016**, *6*, 3. [CrossRef]

128. Halverson, H.; Bausano, J.; Case, S.; Lesko, J. Simulation of Response of Composite Structures under Fire Exposure. *Sci. Eng. Compos. Mater.* **2005**, *12*, 93–102. [CrossRef]